Dissolution behaviour of ULC steel in carbon saturated hot metal

edited by: **F. M. Penz, J. Schenk, R. Ammer, K. Pastucha, B. Maunz**

In addition to hot metal, the Linz-Donawitz oxygen steelmaking process (LD) uses scrap as an iron source. Aside from this fact, scrap acts as a coolant for the exothermic reactions inside the LD converter and will be dissolved in the hot metal. The optimization of the LD process is also focussed on the thermodynamic and kinetic modelling where literature-based dissolution equations are used. In laboratory scale experiments the dissolution behaviour of ULC steel scrap in hot metal with two different carbon concentrations was investigated. For the evaluation of the experiments, a literature model for diffusive melting of scrap in hot metal was examined. Based on the measured ablation rate of cylindrical scrap samples submerged in hot metal, the mass transfer coefficient for the dissolution of ULC steel was determined.

KEYWORDS: BASIC OXYGEN FURNACE – STEELMAKING – SCRAP DISSOLUTION – THERMODYNAMICS –PROCESS MODELLING

Florian Markus Penz
K1-MET GmbH, Linz, Austria;

Johannes Schenk
K1-MET GmbH, Linz & Chair of Ferrous Metallurgy Montanuniversitaet Leoben, Austria;

Rainer Ammer
voestalpine Stahl GmbH, Linz, Austria;

Krzysztof Pastucha
Primetals Technologies Austria GmbH, Linz, Austria;

Bernhard Maunz
voestalpine Stahl Donawitz GmbH, Donawitz, Austria;

INTRODUCTION

Oxygen steelmaking in an LD converter was developed in the early 1950s in Linz and Donawitz (LD) and it gradually became the most dominant method of crude steel production. Large quantities of scrap are used for an ordinary blowing process in an LD converter besides hot metal, which is the main charging material. Scrap is mainly used as a coolant for the process due to heat generation from the oxidation reactions of carbon, silicon, manganese and phosphorus. The dissolution and melting behaviour of scrap influences the whole process cycle in the converter. Many articles concerning the scrap melting process have been published in the past, whereby only a few describe the kinetics of a special steel scrap like ULC in hot metal with changing carbon content. (1 - 12) In this work, an experimental investigation of the melting behaviour of ULC (ultra-low carbon) steel scrap in hot metal with different carbon content was executed. The experiments are based on thermodynamic and kinetic calculations through a MatLab® coded single-zone LD model. Detailed descriptions of the model are published in (13 - 16). In previous calculations it was shown that low alloyed scrap types tend toward a stagnation of dissolution and melting during the oxygen blowing process using literature-based analytical equations (15). Based on these results, laboratory scale experiments were done for validation.

DERIVATIONS OF THE OBSERVED DATA

A collection of measurement data from LD-converters by various authors on the carbon concentration of the molten steel and the melt temperature during the blowing process is presented in (3). It was found that the change of the carbon content is a function of the melt temperature and its trend is parallel to
the liquidus line (austenite-liquid melt) in the Fe Fe_3C phase diagram. Most of the data points are in the liquid phase but some are in the two-phase area of austenite and liquid melt. A similar behaviour is also modelled with the LD model used and was partly published in (15). To describe the scrap melting and dissolution behaviour following literature-based considerations were applied.

The literature describes the melting of scrap in different phases where the diffusion process of carbon controls the scrap dissolution as long as the metal phase temperature is below the melting point of the scrap. If the temperature exceeds the melting point of the scrap a model for forced scrap melting is used. The scrap melting point is defined by the liquidus temperature in the phase diagram for the given chemical composition of the scrap.
The rate of diffusive melting of scrap is determined by the diffusive mass transport of carbon between the liquid metal and the charged scrap. Equation [1] is a mathematical model, proposed by Zhang L. and F. Oeters (6), where the mass transfer coefficient k_{met} in [m s^{-1}] is a decisive factor.

$$-\frac{\partial r}{\partial t} = k_{met} * \ln\left(\frac{\%C_{Scrap} - \%C_{HM}}{\%C_{Scrap} - \%C_{liq}}\right) \quad (1)$$

The scrap particles are assumed as spheres in the model used and the radius of the particle is r in unit [m]. C_{scrap} and C_{HM} are the carbon concentrations in the scrap and hot metal in [wt.-%]. C_{liq} describes the carbon concentration of the scrap on the liquidus line at a given temperature. (6) In this work, the liquidus line was determined for the actual silicon and manganese content of the scrap using the Fe-Fe_3C phase diagram generated by the FactSageTM FSstel database. (13, 15, 17)
When the temperature exceeds the scrap melting point, forced or convective scrap melting starts, where the mass transfer could be neglected since the heat transfer becomes dominant for the dissolution process. (5, 6, 18) In comparison to diffusive scrap melting, the driving force the temperature difference between scrap and hot metal during forces scrap melting. The equation for the forced scrap melting is cited in other publications. (15, 16) Forced scrap melting is not relevant for this research work, since the melting point of the ULC scrap was above the hot metal temperature in all experiments.

DESCRIPTION OF EXPERIMENTS

Dissolution tests

For the experimental procedure, an alumina crucible was charged with 320 g to 345 g of hot metal and positioned in a high temperature vertical tube furnace. The heating rate was 300 K/min to reach the starting temperatures, which are listed in Tab. 1. Before the first and between each further dissolution experiment, a holding time of 30 min was set. To prevent oxidation of the hot metal, the vertical tube furnace was flushed with nitrogen during the heating and melting process. The scrap geometry was cylindrical with a diameter of 12 mm and a length of 30 mm. The whole specimen, including the sample holding, is shown in Fig. 1. The cylinder was submerged into the hot metal with a depth of 20 mm, whereby the axial heat flow to the specimen holding was diminished through a notch. The starting temperature of the specimen was 25 °C. The axial movement of the cylinder to the melt was carried out with a vertical pneumatic controlled cylinder. No stirring by rotation of the cylinder or crucible was performed during the dissolution experiment (i.e. static conditions).

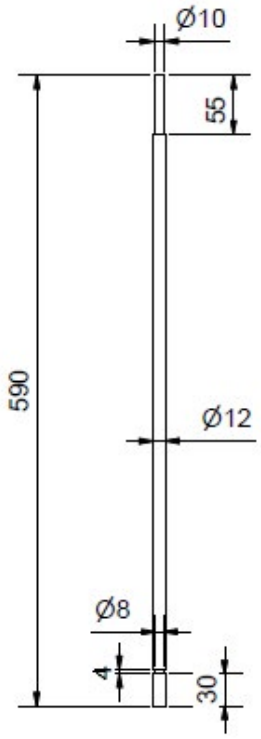

Fig. 1 - Sample geometry including the sample holding part (units in mm)

Before each dissolution experiment, the mass of the cylinder was determined. After a defined dissolution time, the cylinder was extracted from the melt and immediately quenched with water to inhibit further carbon diffusion in the sample and weight change by oxidation with air. Through the mass difference (Δm), the ablation rate of the radius Δr/Δt was evaluated. For this evaluation, the density of the cylinder, defined by equation [2], was used and assumed to be equal at the equilibrium temperature. After the experiments, it was observed that only a melting in radial direction occurred. Local density differences can explain this according to the temperature gradient in the boundary layer of the hot metal. The denser liquid will move downwards along the cylinder surface and inhibit a melting on the bottom surface of the cylinder, which is why the length of the cylinder remains nearly constant in all experiments.

The density of the scrap $\boldsymbol{\rho_{scr}}$ is defined by equation [2] published by Miettinen in (19) and is dependent on the temperature (in °C) and the scrap composition. The scrap is assumed to be ferritic and the density for a multicomponent system (composition $\boldsymbol{C_{i,scr}}$ in wt.-%) is, according to the considered elements i of the scrap, explained with equation [2]. (19)

$$\rho_{scr} = 7875.96 - 0.297T - 5.62 * 10^{-5}T^2 + (-206.35 + 0.00778T + 1.472 * 10^{-6}T^2) * C_{C,scr} + 36.86 * C_{Si,scr} - 30.78 * C_{Mn,scr} \quad \textbf{(2)}$$

The compositions of the hot metal and scrap samples used in the experiments are listed in Tab. 1 and Tab. 2, respectively. The dissolution tests were executed with ULC scrap in carbon saturated hot metal (hot metal 1) at three different temperatures (experiment numbers 1 to 3). Experiment number 4 was executed with hot metal 2 (carbon content of 1 wt.-%), which has a composition close to the liquidus line of the ULC at 1443 °C. The starting temperature of the experiment was assumed to be 1550 °C according to the calculation of the equilibrium temperature, which will be explained subsequently. According to Zhang and Oeters' model, a stagnation of the melting behaviour should occur when the driving concentration difference ($\%Cs_{crap}$ - $\%C_{liq}$) in equation [1] should become zero.

Tab. 1 – Hot metal specification

	Hot metal specification			
	Hot metal 1			Hot metal 2
Carbon content [wt.-%]	4.58			1
Silicon content [wt.-%]	0.37			0.1
Manganese content [wt.-%]	0.63			0.161
Phosphorus content [wt.-%]	0.07			0.015
Mass of hot metal [g]	320			345
Starting temperature [°C]	1305	1370	1450	1550
Experiment number [-]	1	2	3	4

Tab. 2 – Scrap specification

Scrap specification		
	ULC scrap	S235JR
Carbon content [wt.-%]	0.002	0.1
Silicon content [wt.-%]	<0.001	0.0733
Manganese content [wt.-%]	0.05	0.479
Phosphorus content [wt.-%]	0.003	0.01
Mass of hot metal [g]	26.3	26.3
Starting temperature [°C]	25	25
Experiment number [-]	1-4	Pre-test

Pre-Tests for Verification of Starting Conditions

Before the dissolution experiments, pre-tests were executed to verify the starting conditions for the individual dissolution tests. The starting temperature of the melt was measured with a thermocouple type B, which was directly submerged into the melt. This temperature is shown in Tab. 1 for experiments 1 to 4.

In a preceding test series of this research work, the melting and dissolution behaviour of S235JR scrap was investigated. In the course of this investigation, S235JR specimens (see Tab. 2) were used for verification of the equilibrium temperature between the liquid metal and the submerged sample, which results from the heat exchange between hot melt and cold scrap. For this purpose, a thermocouple type S was located in a bore with a diameter of 1.7 mm in the cylinder centre and at a distance of 10 mm from the cylinder tip. The cold cylinder was submerged into the liquid hot metal and the temperature was monitored until the equilibrium between the melt and the cylinder was reached. This temperature was always below the starting temperature of the hot metal, according to Tab. 1. The S235JR has a very similar enthalpy to ULC steel as a function of temperature. Fig. 2 shows these functions for ULC steel and S235JR, calculated with the FactSageTM FSstel and FactPS database. Accordingly, it was assumed that the equilibrium temperature measured for S235JR should be the same as for ULC steel.

The equilibrium temperature was evaluated with a heat balance, based on equations [3] and [4]. Whereas mScrap and mhot metal are the masses of the scrap and the hot metal in [kg], Q is the heat flux in [W m^{-2}], cp,hot metal is the specific heat capacity in [J kg^{-1} K^{-1}], $T_{start\ scrap/hot\ metal}$ and $T_{equilibrium}$ are the starting temperature of the melt or scrap and the equilibrium temperature in [K]. $H_{Scrap}(T)$ is the temperature dependent enthalpy in [J kg^{-1}]. For the determination of Tequilibrium, the heat fluxes of the scrap and hot metal must be equal. (20)

$$Q_{Scrap} = m_{scrap} * (H_{Scrap}(T_{equilibrium}) - H_{Scrap}(T_{start\ scrap}) \quad (3)$$

$$Q_{Hot\ metal} = m_{hot\ metal} * c_{p,hot\ metal} * (T_{equilibrium} - T_{start\ hot\ metal}) \quad (4)$$

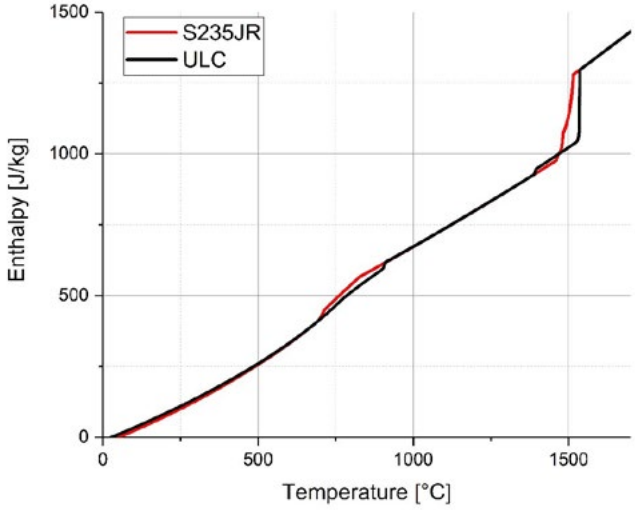

Fig. 2 - Enthalpy of ULC steel and S235JR

DISCUSSION AND RESULTS

The increase in the scrap core temperature based on the four investigated starting temperatures of the melt is shown in Fig. 3.

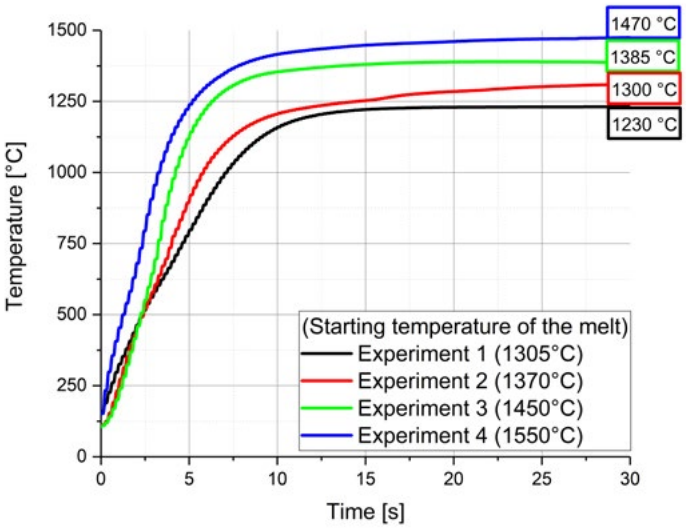

Fig. 3 - Measurement of the core temperature in the cylinder centre and equilibrium temperature

As seen in Fig. 3, the equilibrium temperature is reached within 10 seconds. The higher the starting temperature, the steeper the temperature gradient is. The measurement also shows that the equilibrium temperature is 65 °C to 80 °C below the starting temperature of the melt. In Tab. 3 the measured starting and equilibrium temperatures of the hot metal and the scrap are listed and compared with the calculated equilibrium temperatures from the heat balance obtained from equations [3] and [4] as well as the data from Fig. 3.

Tab. 3 – Starting and equilibrium temperatures of the hot metal and the scrap

Starting and equilibrium temperatures					
	Starting temperature melt[°C]	Starting temperature scrap[°C]	Equilibrium temperature calculated[°C]	Equilibrium temperature measured [°C]	Temperature drop measured [°C]
Experiment 1	1305	25	1239	1230	75
Experiment 2	1370	25	1301	1300	70
Experiment 3	1450	25	1377	1385	65
Experiment 4	1550	25	1452	1470	80

Based on the well-fitting results of the thermocouple measurements, the determination of heat transfer coefficient k_{met} according to equation [1] becomes possible. In the following phase diagram (Fig. 4) of the present ULC scrap, the measurement points according to the hot metal composition (magenta) and the temperature development of experiment 4 with a carbon content of 1 wt.-% are shown. The blue line indicates the way of the equilibrium temperature between 10 to 30 s., whereby the liquidus line is exceeded during this time. Such behaviour does not occur during the experiment with hot metal with 4.58 wt. % carbon. For each equilibrium temperature, the carbon concentration on the liquidus line (cliq) in the Fe-Fe_3C phase diagram was determined. The terms of the carbon differences from equation [1] for each experiment are presented in Tab. 4.

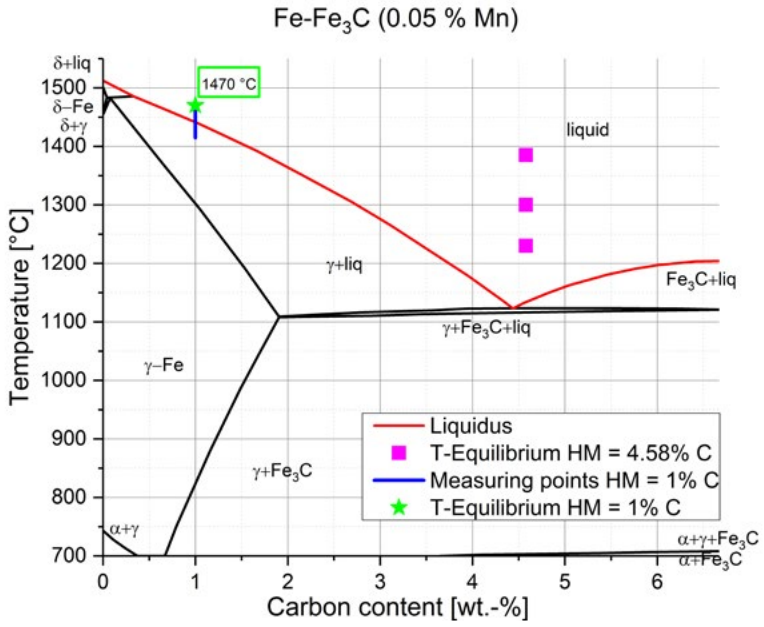

Fig. 4 - Measured equilibrium temperature based on the present ULC scrap composition phase diagram

Tab. 4 – Carbon differences based on equation [1]

Carbon differences of equation 1			
	Equilibrium temperature [°C]	(%Cscrap - %Cliq) [wt.-%]	(%Cscrap - %CHM) [wt.-%]
Experiment 1	1230	-3.4651	-4.5763
Experiment 2	1300	-2.7467	-4.5763
Experiment 3	1385	-1.7612	-4.5763
Experiment 4	1470	-0.5930	-0.9980

The experimental determination of the ablation rate of the radius (Δr/Δt) for experiments 1 to 3, executed in hot metal with a carbon content of 4.58 wt.-%, is presented in Fig. 5.

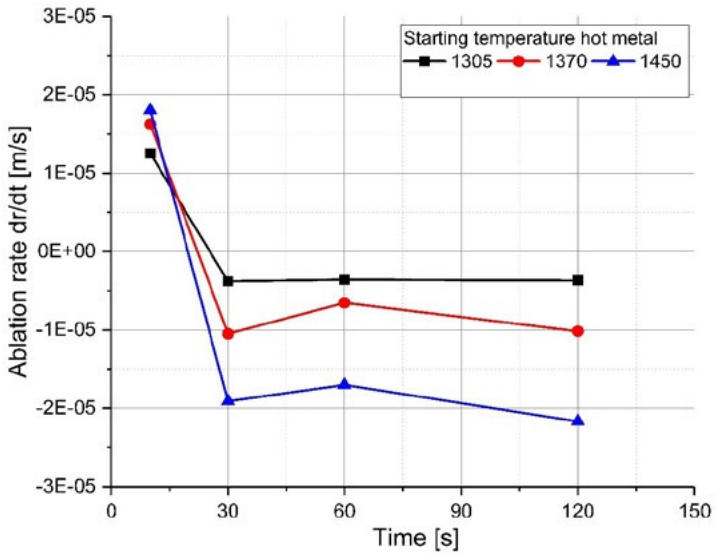

Fig. 5 - Ablation rate of ULC steel scrap in carbon saturated hot metal

At the beginning of the process, a positive ablation rate occurs. This phenomenon is attributed to a shell formation due to solidification of the liquid hot metal on the cold scrap surface. After a certain progressing time, the turning point is reached, the shell formation stops, and the melting of the shell starts. When the ablation rate turns negative, the melting of the mother scrap starts. The melting and dissolution is dependent on the equilibrium temperature, which is reached in this case, according to the measurements in Fig. 3, after 10 s. By using equation [1] the mass transfer coefficient for this system is calculated. According to the negative sign in the equation, a positive heat transfer is expected if the melting of the mother scrap is in progress. In Fig. 6 the calculated mass transfers of the three starting temperatures are plotted. As mentioned, the mass transfer is negative during the growth and melting of the shell layer at the beginning of the process and becomes positive after 25 s dissolution time at the latest. According to the progress, it could be established that the mass transfer coefficient will increase slightly with the temperature after the equilibrium temperature has been reached.

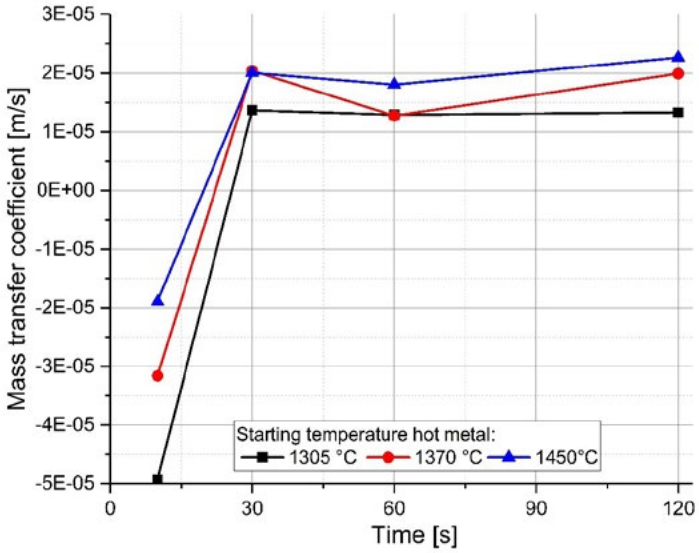

Fig. 6 - Experimental mass transfer coefficient

During the LD-process, the carbon content in the liquid melt decreases and the temperature increases in line with the exothermic reactions of oxidation. Therefore, the melting behaviour of ULC steel scrap was determined in modified hot metal with 1 % C. In Fig. 7 the mass transfer coefficient and the ablation rate of experiment 4 are presented. According to the heat balance calculation and measurement the specimen temperature increases to 1415 °C after 10 s and 1470 °C after 30 s, which is just above the liquidus line in the quasi-binary phase diagram..

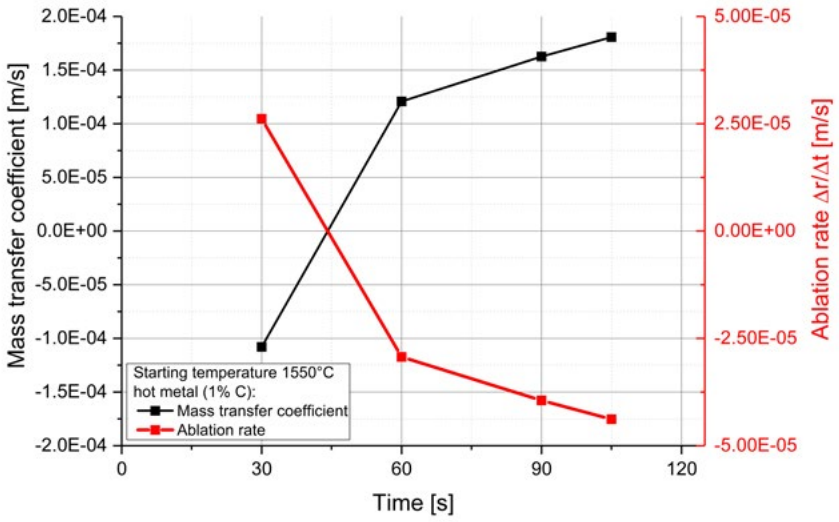

Fig. 7 - Mass transfer coefficient and ablation rate of ULC scrap in hot metal containing 1 %C

The smaller carbon content in the hot metal results in a strong shell formation at the beginning of the process with a higher negative mass transfer coefficient in comparison to experiments 1 to 3, with higher carbon contents in the hot metal. However, under real process conditions, shell formation will not occur. The scrap will be, due to heat conduction, almost at the equilibrium temperature when those amounts of carbon are reached. This will result in a higher expected negative mass transfer coefficient with an approach to 0. For that reason, a stagnation of the melting behaviour, described by equation [1], where the driving of (%Cscrap - %Cliq) would become zero or negative could be neglected. An explanatory argument is therefore that in this measurement just above the liquidus line, a dissolution of the ULC steel with high mass transfers occurs, which would not be stopped immediately when reaching the liquidus line or ends in an abrupt negative mass transfer coefficient when the temperature falls below the liquidus line.

CONCLUSION

This publication presents the results of laboratory scale experiments on the dissolution and melting behaviour of ULC steel scrap in hot metal with two different carbon concentrations.
For the investigation, four different experiments with various hot metal temperatures were performed. For the evaluation of the hot metal mass transfer coefficient of the diffusive scrap melting process, a literature-based equation was used. To get the true process equilibrium temperature, a pre-test with a thermocouple in the core position of the specimen was executed, resulting in a temperature drop of more than 65 °C. Based on these measurements, the carbon concentrations on the liquidus line of the current available Fe-Fe_3C-Mn phase diagram were evaluated. With the measurements, the ablation rates of the radius were determinable and furthermore, the mass transfer coefficients were defined. What is mentionable is that the mass transfer coefficient is slightly dependent on the temperature. At the beginning of the process a shell formation occurs, which results in a negative mass transfer. If the carbon content in the melt decreases and the temperature increases, an increase in the mass transfer is observable. This results in a high melting rate of ULC scrap just above the liquidus line which would not turn into an abrupt negative mass transfer coefficient if the liquidus line were undercut.
In summary, the outcomes of this work clearly indicate that the actual temperature and melt composition have a strong impact on the melting and dissolution behaviour of ULC steel scrap. However, the difference in the dissolution behaviour of hot metal with 4.58 and 1 wt.-% carbon is not fully explainable. More research work must be done to investigate and describe the melting and dissolution of scrap for the conditions in the LD process.

ACKNOLEDGMENT

The authors gratefully acknowledge the funding support of K1-MET GmbH, metallurgical competence centre. The research programme of the K1-MET competence centre is supported by COMET (Competence Centre for Excellent Technologies), the Austrian programme for competence centres. COMET is funded by the Federal Ministry for Transport, Innovation and Technology, the Federal Ministry for Science, Research and Economy, the provinces of Upper Austria, Tyrol and Styria as well as the Styrian Business Promotion Agency (SFG).

REFERENCES

[1] Turkdogan ET. Fundamentals of steelmaking. The institute of materials. London. 1996.

[2] Ghosh A, Chatterjee A. Ironmaking and Steelmaking theory and practice. PHI Learning Private Limited. Delhi. 2015.

[3] Asai S, Muchi I. Effect of scrap melting on the process variables in LD converter caused by the change of operating conditions. Transactions ISIJ. Vol. 11; 1971. p. 107 – 115.

[4] Gaye H, Wanin M, Gugliermina P, Schittly Ph. Kinetics of scrap dissolution in the converter. Theoretical model and plant experimentation. 68th Steelmaking conference, AIME, Detroit, USA. 1985. p. 91 – 103

[5] Isobe K, Maede H, Ozawa K, Umezawa K, Saito C. Analysis of the scrap melting rate in high carbon molten iron. ISIJ. Vol. 76; No.11, 1990. p 2033 – 2040.

[6] Zhang L, Oeters F. Schmelzen und Mischen von Legierungsstoffen in Stahlschmelzen. Verlag Stahleisen GmbH. Düsseldorf. 2012.

[7] Szekely J, Chuang YK, Hlinka JW. The melting and dissolution of low-carbon steels in iron-carbon melts. Metallurgical Transactions; Vol. 3; 1972. p. 2825 – 2833.

[8] Shukla AK, Deo B, Robertson DGC. Scrap Dissolution in Molten Iron Containing Carbon for the Case of Coupled Heat and Mass Transfer Control. Metallurgical and Materials Transactions B; Vol. 44; 2013. p. 1407 – 1427.

[9] Den Hartog HW, Kreyger PJ, Snoeijer AB. Dynamic model of the dissolution of scrap in BOF process. C.R.M. Rep. Vol. 37; No. 12, 1973. p. 13 – 22.

[10] Kawakami M, Takatani K, Brabie LC. Heat and Mass Transfer Analysis of Scrap Melting in Steel Bath, Tetsu-to-Hagané. Vol. 85; No. 9, 1999. p. 658 – 665.

[11] Kruskopf A, Holappa. Scrap melting model for steel converter founded on interfacial solid/liquid phenomena. Metallurgical Research and Technology. Vol. 115; 2018. p. 201 – 208.

[12] Sethi G, Shukla AK, Das PC, Chandra P, Deo B. Theoretical Aspects of Scrap Dissolution in Oxygen Steelmaking Converters. AISTech 2004 Proceedings Volume II, Nashville, USA. 2014. p. 915 – 926.

[13] Lytvynyuk Y, Schenk J, Hiebler M, Sormann A. Thermodynamic and Kinetic Model of the Converter Steelmaking Process. Part 1: The Description of the BOF Model. Steel Research int. Vol. 85; No. 4, 2014. p. 537 – 543.

[14] Bundschuh P. Thermodynamische und kinetische Modellierung von LD-Konvertern. Dissertation. Montanuniversität Leoben, Austria. 2017.

[15] Penz FM, Bundschuh P, Schenk J, Panhofer H, Pastucha K, Paul A. Effect of Scrap Composition on the Thermodynamics of Kinetic Modelling of BOF Converter. 2nd VDEh-ISIJ-JK Symposium, Stockholm, Sweden. 2017.

[16] Penz FM, Bundschuh P, Schenk J, Panhofer H, Pastucha K, Paul A. Impact of Carbon, Silicon and Manganese contents on the dissolution and melting behaviour of scrap in a dynamic BOF model. 3rd European steel technology and application days (ESTAD), Vienna, Austria. 2017.

[17] Zarl M. Development and evaluation of a BOF pre-processor model. Master Thesis. Montanuniversität Leoben, Austria. 2017.

[18] Boychenko B, Okhotskiy V, Kharlashin P. The converter Steelmaking. Dnipro-VAL, Dnipropetrovsk. 2006.

[19] Miettinen J. Calculation of solidification-related thermophysical properties for steels. Metallurgical and materials transactions B. Vol. 28 B; No. 4, 1997. p. 281 – 297.

[20] Seshadri V., Tavares Parreiras R., Da Silva C.A., Da Silva I.A. Transport phenomena: fundamentals and applications in Metallurgical and Materials Engineering. ABM, Sao Paulo. 2011.